AGU PUBLICATIONS

JGR

Journal of Geophysical Research: Space Physics

RESEARCH ARTICLE
10.1002/2017JA024786

Key Points:
- Antennas on spacecraft are poor collectors of charge from dust impact plasmas
- The analysis of the waveforms supported by laboratory simulations will help to understand how dust impact signals are generated
- There is a wide variety of S/WAVES dust signals that need explanation

Correspondence to:
Z. Sternovsky,
zoltan.sternovsky@colorado.edu

Citation:
O'Shea, E., Sternovsky, Z., & Malaspina, D. M. (2017). Interpreting dust impact signals detected by the STEREO spacecraft. *Journal of Geophysical Research: Space Physics*, *122*. https://doi.org/10.1002/2017JA024786

Received 14 SEP 2017
Accepted 28 NOV 2017
Accepted article online 4 DEC 2017

Interpreting Dust Impact Signals Detected by the STEREO Spacecraft

E. O'Shea[1,2], Z. Sternovsky[2,3,4], and D. M. Malaspina[2]

[1]Department of Physics, University of New Hampshire, Durham, NH, USA, [2]LASP, University of Colorado, Boulder, CO, USA, [3]Smead Aerospace Engineering Sciences, University of Colorado, Boulder, CO, USA, [4]IMPACT, University of Colorado, Boulder, CO, USA

Abstract There is no comprehensive understanding yet of how dust impacts on spacecraft (SC) generate signals detected by antenna instruments. The high sensitivity of the S/WAVES instrument and the large number and high diversity of dust impacts detected make the STEREO mission particularly well suited for a closer investigation. A floating perturbation model (FPP) was recently proposed to explain the characteristic shape of dust impact signals with an overshoot. The FPP model posits that the overshoot is due to the different discharge time constant of the SC and the individual antennas. Kinetic simulations are performed to demonstrate that, contrary to common belief, antennas are inefficient collectors of charged particles from impact plasmas. The collection efficiency is small, only 0.1–1%, varying weakly with the bias potential between the antenna and the SC, and more strongly with impact location. The low recollection efficiencies and an analysis of the shapes and scaling of typical and atypical signals recorded by S/WAVES suggest that, besides the mechanism described by the FPP model, there is another, possibly stronger mechanism that is responsible for generating the characteristic overshoot for most dust impact signals observed by STEREO.

1. Introduction

The detection of cosmic dust using antenna instruments in space dates back to the Voyager missions and their visits to Saturn, Uranus, and Neptune (Aubier, Meyer-Vernet, & Pedersen, 1983; Gurnett et al., 1983, 1991; Meyer-Vernet, Aubier, & Pedersen, 1986; Pedersen et al., 1991). The Cassini spacecraft has been detecting dust impacts around Saturn using both antennas (Kurth et al., 2006; Wang et al., 2006; Ye et al., 2014; Ye et al., 2016; Ye, Gurnett, & Kurth, 2016) and a dedicated dust instrument (Kempf, 2008). The S/WAVES plasma wave antenna instruments on the two STEREO (Solar Terrestrial Relations Observatory) spacecraft on their orbit about the Sun are also sensitive to impacts of cosmic dust (Bale et al., 2008; Bougeret et al., 2008). The S/WAVES observations are unique in that they provided an unexpectedly large number and wide variety of transient signals associated with dust impacts. One class of these voltage pulses, known as "single-hits," was interpreted as being due to nanometer-seized dust particles impacting the spacecraft (SC) with high velocities (Meyer-Vernet et al., 2009). These "nanodust" particles are generated near the Sun by collisional processes and accelerated by the expanding solar wind plasma (Czechowski & Mann, 2010; Juhász & Horányi, 2013; O'Brien et al., 2017). Another subset of the STEREO dust data, known as "triple-hits," was interpreted as due to interplanetary and interstellar dust particles impacting the SC body. Zaslavsky et al. (2012) have shown that the yearly variation of the triple-hit events is consistent with a yearly modulation of the interstellar dust flux. Malaspina et al. (2015) extended the observational period and refined the analysis by using more relevant laboratory calibration data for the generated impact charge, ultimately reaching the same conclusions as Zaslavsky et al. (2012). Recently, Kellogg, Goetz, and Monson (2016) performed a detailed qualitative analysis of the dust impact signals detected by the Wind satellite and a comparison between the Wind and STEREO observations. The reader is pointed to this work for a more detailed discussion of a number of interesting features in the interpretation of dust impact signals.

There is little doubt that the impacts of cosmic dust particles can generate measurable signal on antennas. Hypervelocity impacts of particles on solid surfaces generate small plasma puffs, also known as impact plasmas. Following the work by Oberc (1996), there are three basic mechanisms that can lead to the generation of transient voltage signals: (1) charge recollection on the SC body, (2) charge recollection on the antenna(s), and (3) exposure of the antenna to the fields generated by the expanding plasma cloud. Recent laboratory simulations have followed up on the signal generation mechanisms using simplified and reduced-size setups. Collette et al. (2015) have confirmed that charge recollection by the SC and antennas are valid mechanisms

and that the polarity and amplitude of the generated signals depend not only on the total generated impact charge but also on the applied bias voltages. Charging mechanism (3) from above was not observed during the laboratory investigations; however, a new mechanism was identified: A transient signal can be generated as an induced (or image) charge from the electron and ion clouds originating from the impact plasma and separated due to their vastly different thermal speeds. (This mechanism is clearly identified in the S/WAVES data as well, see section 3 below.) Nouzák et al. (2017) performed the first laboratory simulation measurements for both monopole and dipole antenna configurations and confirmed and expanded upon the findings by Collette et al. (2015). Collette et al. (2014) have characterized impact charge generation for STEREO-relevant materials using the equation $Q = \alpha m v^{\beta}$, where Q is the charge of the generated impact plasma, m and v are the mass and velocity of the dust particle, and α and β are fitting parameters that are characteristic to each target material. Collette, Malaspina, and Sternovsky (2016) measured the temperatures of the electron and ion components of the impact plasma and found that that of the former is on the order of a few eV and does not change significantly with impact velocity. The ion temperature, on the other hand, increases from about 5 eV at low impact speeds ($<$10 km/s) to 20–30 eV at impact speeds of 20 km/s and higher. Impact charge yields and plasma temperatures measured in the laboratory are useful for interpreting antenna measurements in space, as these are needed to relate dust mass to the generated impact charge, and then, in turn, for estimating the fraction of impact charge recollected by the SC and antennas. From their detailed analysis of the Wind dust impact data, Kellogg et al. (2016) concluded that the dominant signal generation mechanism depends on the configuration (monopole versus dipole) of the antennas.

Despite these successes and others, a persistent lack of detailed understanding of the physical mechanisms responsible for producing the dust-impact voltage signal on electric field antennas limits the usefulness of these impact signals for characterizing dust populations. For example, it was demonstrated recently for individual waveforms captured by Cassini that antennas operated in a dipole mode are greatly insensitive to dust impacts occurring on the SC body, and only direct antenna hits are registered in this mode (Ye et al., 2016). Though this concept was established in the context of Wind spacecraft data by Meyer-Vernet et al. (2014) and Kellogg et al. (2016). The mode of antenna operation is important, as the effective impact area and sensitivity are rather different for the different operational modes and these quantities are needed to calculate the flux of dust particles and their mass. Nouzák et al. (2017) confirmed the insensitivity of dipole antennas to SC impacts in laboratory conditions using a scaled down model of the Cassini spacecraft.

The shape and polarity of individual dust impact events can also reveal details of the physical processes that generated the signal. For example, the S/WAVES events registered in the time domain mode often show a sharper peak followed by a longer overshoot of an opposite polarity. Zaslavsky (2015) proposed that these complex shapes of the dust impact signals can be explained by taking into account the different discharge time constants of the SC and the antenna. The antenna potential is measured relative to the SC, and the difference of the two temporally evolving signals can reproduce the overshoot effect. Based on this model, Thayer et al. (2016) performed an analysis on a carefully selected subset of the S/WAVES data and showed that the amplitude of the overshoot does increase with increasing positive bias of the antenna with respect to that of the SC. However, such behavior was observed only for two antennas, while one antenna showed opposite correlation, possibly due to uneven exposure to UV illumination. The purpose of this article is to revisit the S/WAVES dust impact data and investigate whether the FPP model alone is sufficient to explain observed common and less common signal shapes. A simple numerical model is also presented that calculates the recollected fraction of the impact-generated electrons by the antennas. The results show that this fraction is much smaller than assumed by the FPP model.

The article is structured as follows: section 2 is a brief review of the FPP model. Section 3 presents some of the common and less common features observed in the data set from STEREO with a statistical analysis. The numerical model of charge recollection calculations is presented in section 4. Section 5 is the summary of the results and conclusion.

2. Review of the Floating Potential Perturbation (FPP) Model

Here we present and rederive the fundamentals of the FPP model that loosely follows the original work by Zaslavsky (2015). The STEREO spacecraft operate near 1 AU in interplanetary space, where photoelectron

emission due to solar UV radiation dominates SC surface charging. A positive equilibrium potential establishes both on the SC and the antenna that satisfies the following equation:

$$C_x \frac{d\varphi_x}{dt} = I_{\mathrm{ph},x} + I_{e,x} = 0, \tag{1}$$

where C is capacitance, φ is potential, and I_{ph} and I_e are the emitted photoelectron current and electron current collected from the solar wind plasma, respectively. Solar wind ions and secondary electron currents are negligibly small in this environment. Subscript x referrers to either SC or antenna. The charging currents are given by the following equations:

$$I_{\mathrm{ph},x} = S_{\mathrm{ph},x}\, J_{\mathrm{ph},0} \exp\left(-\frac{\varphi_x}{T_{\mathrm{ph}}}\right), \tag{2}$$

$$I_{e,x} = -S_x\, J_{e,0} \left(1 + \frac{\varphi_x}{T_e}\right)^{g_x}, \tag{3}$$

where S_x and $S_{\mathrm{ph},\,x}$ are the surface area of element x and surface area exposed to sunlight, respectively. $T_{\mathrm{ph}} \approx 2$ eV and $T_e \approx 8$ eV are typical temperatures of photo- and solar wind electrons, respectively, expressed in units of eV. $J_{\mathrm{ph},\,0} = 20 - 50\ \mu\mathrm{A/m}^2$ is the photoelectron current density that can vary over a wide range depending on solar activity (Sternovsky et al., 2008), and $J_{e,\,0} = e_0 n_e w_e$ is the kinetic current flux of solar wind electrons with $w_e = \sqrt{e_0 T_e / 2\pi m_e}$, where m_e is electron mass, n_e is the undisturbed solar wind density, and e_0 is the elementary charge. The geometric factor, $g_x = 0, \frac{1}{2}$, or 1, depending on the symmetry of the system and is applicable for the 1-D, cylindrical, and spherical cases, respectively. The minus sign in equation (3) indicates the collection of electrons.

The floating (equilibrium) potential of the antenna and SC can be calculated using equation (1) and for typical solar wind plasma conditions is on the order of +6 V. Antennas, due to their geometry, are less effective in collecting solar wind electrons and can float 0.5–1 V more positive than the SC.

During a dust impact, charge Q_x is recollected by element x from the impact plasma cloud, which results in a small deviation from the floating potential with a peak value of

$$\delta V_x = \frac{Q_x}{C_x} \tag{4}$$

where the capacitances of elements are estimated to be $C_{\mathrm{SC}} = 200$ pF and $C_{\mathrm{ant}} = 60$ pF (Zaslavsky, 2015). The voltage pulse has a characteristic temporal evolution that can be estimated as follows. The risetime of the pulse is determined by generation of the dust impact plasma and charge recollection. Both of these processes are fast (on the order of ~10 μs) relative to other time constants. After charge collection, the element will discharge through the ambient plasma and return to the equilibrium potential. The characteristic time constant of this discharge can be calculated as $\tau_x = -C_x \delta V_x / I_{\mathrm{dis},\,x}$, where the net discharge current is $I_{\mathrm{dis},\,x}(\varphi_x) = (I_{\mathrm{ph},x}(\varphi_x) + I_{e,x}(\varphi_x))$. The minus sign in the former relation indicates that the voltage variation and the restoring discharge current have opposite polarities. Near the equilibrium potential the discharge current is small, $I_{\mathrm{dis},x}(\varphi_{\mathrm{eq},x}) \approx 0$, and is best expressed in a differential form to obtain an expression for the time constant as

$$\tau_x = -C_x \frac{\delta V_x}{\left.\frac{dI_{\mathrm{dis},x}}{d\varphi_x}\right|_{\varphi_{\mathrm{eq},x}} \delta V_x} = \frac{-C_x}{\left.\frac{dI_{\mathrm{dis},x}}{d\varphi_x}\right|_{\varphi_{\mathrm{eq},x}}} \tag{5}$$

This expression is now independent on the magnitude of the voltage variation. Assuming a 1-D case for the SC ($g = 0$),

$$\frac{dI_{\mathrm{dis,SC}}}{d\varphi_{\mathrm{SC}}} = S_{\mathrm{ph,SC}}\, J_{\mathrm{ph},0} \exp\left(-\frac{\varphi_{\mathrm{SC}}}{T_{\mathrm{ph}}}\right)\left(-\frac{1}{T_{\mathrm{ph}}}\right). \tag{6}$$

Evaluating the derivative at the equilibrium potential, $\varphi_{\mathrm{eq},\,\mathrm{SC}}$, the product of first three terms can be substituted by the expression from equation (3) to obtain

$$\left.\frac{dI_{\mathrm{dis,SC}}}{d\varphi_{\mathrm{SC}}}\right|_{\varphi_{\mathrm{eq,SC}}} = -S_{\mathrm{SC}}\, J_{e,0}\left(\frac{1}{T_{\mathrm{ph}}}\right) \tag{7}$$

that in turn yields the characteristic time constant:

$$\tau_{SC,1D} = \frac{C_{SC} T_{ph}}{e_0 n_e w_e S_{SC}}. \quad (8)$$

This is the same expression as derived in the FPP model by Zaslavsky (2015). However, it is important to realize that the basic assumption of a 1-D charging surface is far from being satisfied as the dimensions of the STEREO SC are smaller than a typical solar wind Debye length of $\lambda_D \approx 10$ m. Using spherical symmetry with $g = 1$ is thus likely more appropriate. The time constant can be calculated similarly to the 1-D case to obtain:

$$\tau_{SC,3D} = \frac{C_{SC} T_{ph}}{e_0 n_e w_e S_{SC}} \frac{T_e}{\left(T_e + \varphi_{eq,SC} + T_{ph}\right)} \cong \frac{1}{2} \tau_{SC,1D} \quad (9)$$

where the approximation on the right takes into account the typical values of electron temperatures and the equilibrium potential for the specific case of the STEREO spacecraft.

Estimating the discharging time constant of the antenna is similar. By simply assuming $g = 1/2$, one can arrive to an approximate expression:

$$\tau_{ant} \cong \frac{C_{ant} T_{ph}}{e_0 n_e w_e S_{ant}} \left(1 + \frac{\varphi_{eq,ant}}{Te}\right)^{-1/2}. \quad (10)$$

Noting, however, that for the cylindrical symmetry to be fully applicable, the antenna length would have to be much larger than the Debye length, which is not the case here. The STEREO antennas are ~6 m long.

It is also interesting to note that the time constants derived above are only weakly dependent on the photoemission current (through the equilibrium potential) and are inversely proportional to the solar wind density. The difference between the discharging times of the SC and the antenna arises from their different surface areas and capacitances. For a typical solar wind density $n_e = 5$ cm^{-3}; electron temperatures, $T_e = 8$ eV, $T_{ph} = 2$ eV; photocurrent density, $J_{ph,0} = 40$ μA/m^2; and spacecraft parameters, $S_{SC} = 10$ m^2, $S_{ph,SC} = 2.5$ m^2, $S_{ant} = 0.5$ m^2, and $S_{ph,ant} = 0.15$ m^2, the solutions to the equations above are $\varphi_{eq,SC} = +5.5$ V, $\varphi_{eq,ant} = +6.4$ V, $\tau_{SC,1D} = 0.106$ ms, $\tau_{SC,3D} = 0.054$ ms, and $\tau_{ant} = 0.49$ ms.

Zaslavsky, 2015 proposed that the characteristic "overshoot" shape of signals that are interpreted as dust impacts on STEREO can be explained by the different discharge time constants of the SC and the antenna. (Figure 1 shows typical dust signals detected by S/WAVES, and the next section provides a more detailed discussion.) The voltage measured between the antennas relative to the spacecraft from the transient event is

$$\delta V_{meas}(t) = \delta V_{ant}(t) - \Gamma \delta V_{SC}(t) \quad (11)$$

The coupling efficiency, Γ, has a value typically somewhere between 0.5 and 1 and accounts for the electric field of the large SC affecting the antenna. $\Gamma = 1$ is assumed hereafter for simplicity. When the dust impact occurs on the SC, electrons from the generated plasma cloud can be collected on SC and the antennas, generating transient negative signals on both. The charge collection is dominated by the SC, which results in the initial positive peak of the measured signal according to equations (4) and (10). The SC then discharges with time constant τ_{SC}. Provided that the antennas collected a sufficiently large fraction of the electrons from the dust impact plasma, the measured voltage may swing negative since the antenna discharge time constant is significantly longer than that of the SC.

The FPP model described above and proposed by Zaslavsky (2015) does appear to be a valid mechanism for producing overshoot signals. However, by the analysis presented below on a variety of S/WAVES signals and supporting modeling calculations, we find sufficient evidence to question whether the FPP model alone can explain the characteristic overshoot signal shapes.

3. Survey of S/WAVES Signal Shapes

The twin STEREO spacecraft orbit the Sun near 1 AU, each equipped with the identical electric field instrumentation (S/WAVES) (Bougeret et al., 2008). Three 6 m long and orthogonally arranged antennas are mounted on the antisunward side with a common base mount. The antennas are operated in a monopole mode and produce multiple data products telemetered back to the ground. The data used in the study

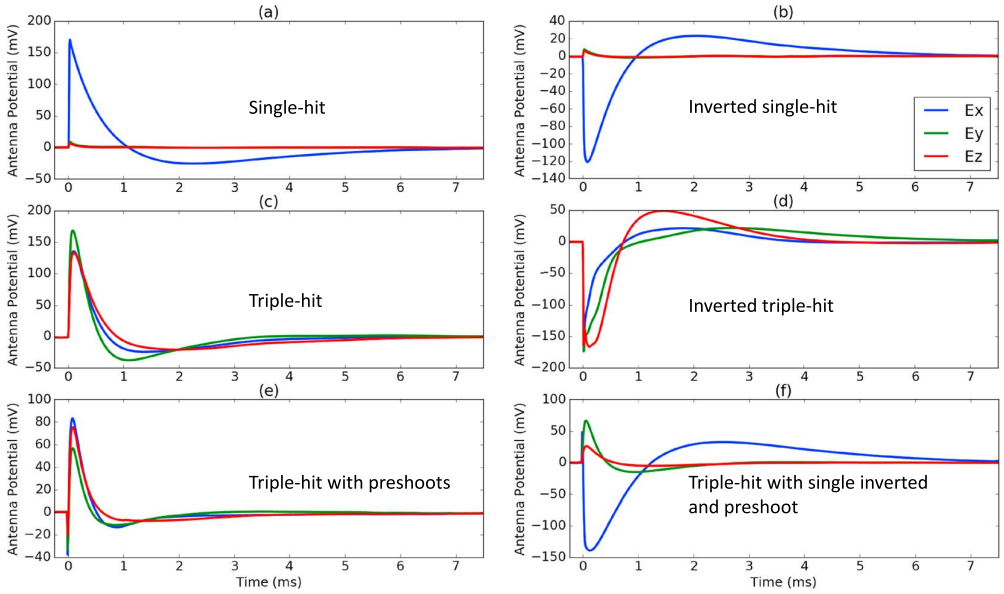

Figure 1. Some of the typical and atypical waveforms recorded by S/WAVES. See text for detail.

below are from the time domain sampler (TDS), which records 65 or 130 ms long time domain waveforms sampled at 256 or 128 kS/s, respectively. The waveforms are continually recorded, and segments with high amplitudes are autonomously selected for telemetry. The TDS data are dominated by characteristic impulsive signals interpreted as dust impacts.

This article attempts to provide some insight into the wide variety of signal shapes recorded by S/WAVES and provide a rudimentary scenario for the generation of some of the observed features. The study is limited to data collected in a single year of 2008 by the STEREO A spacecraft. It is understood that year-to-year variations may exist; nevertheless, the analyzed data set is sufficiently large to represent the diversity of signal shapes. Several limiting conditions were placed on the statistical analysis of the signals presented below. First, only signals with sufficient vertical amplitude ($\geq$10 mV) are included in order to clearly identify their shapes. The analyzed amplitudes are also limited to $<$175 mV in order to avoid effects related to saturation. "Overshoots" are recognized as waveforms that change polarity and reach $\geq$8% of the initial peak's amplitude within 750 μs. "Preshoots" are narrow voltage spikes that occur prior the main peak (within 400 μs) and are at least 10% of the main peak's amplitude. "Inverted signals" are those that have negative-going main peak(s) with an amplitude that is larger than any positive maximum. Figure 1 below presents some of the most common signal shapes identified, followed by a discussion for each.

Single hits (Figure 1a) are the most common signals shapes, and over 79% of the TDS waveforms have this form. The characteristic feature is that one of the antennas detects a signal that is much larger than the others. A possible explanation for these signals, based on the disruption of photoelectron cloud around the antenna by nanodust particle impacts, was proposed by Pantellini et al. (2012) and Zaslavsky et al. (2012). For the purposes of this article, it is important to make two observations: (1) the positive-going signals indicate positive charge collection on the antenna, and the fact that only one antenna is registering a signal indicates that the SC is not recollecting a significant amount of charge. (2) The overshoot on the dominant channel is rather similar to the overshoots of other waveform types presented in Figure 1. A statistical analysis of the data reveals that 99% of single-hit events exhibit overshoots, despite the fact that the mechanisms proposed in the FPP model cannot produce a waveform with the "single-hit" signal characteristics.

Inverted single hits (Figure 1b), approximately 7% of the single-hit signals are inverted with overshoots commonly present. There is currently no good explanation how such signals can be generated, but it is interesting to note that, again, the shape of the overshoots is similar for most detected waveforms.

Triple hits (Figure 1c) are the second most prevalent signal type with close to 20% occurrence. These signals have a straightforward interpretation as being due to impacts on the SC body by interplanetary and interstellar particles. The impact rates and their yearly modulations support this interpretation (Malaspina et al., 2015; Zaslavsky et al., 2012). The risetimes of the main signals shown in this example are on the order of tens of microseconds, which is comparable to the time scales of impact-charge generation and recollection. (The front-end analog electronics and sampling rates are fast in comparison and should not introduce significant distortion.) The discharge time constants range from 0.1 to 0.23 ms with the E_y antenna showing the fastest discharge time. These values are of the same order estimated in section 2. It is indeed reasonable to assume that the discharge is occurring due to recollecting charges by the SC from the plasma environment, and the time constant difference could be due to different solar wind density, solar UV illumination, geometry effects, or the estimated SC capacitance. It is not clear, however, what mechanisms would generate different discharge times for the different antennas.

The next task is to analyze the overshoot effect, which occurs on all three antennas in 99% of the triple-hit signals. The typical relative amplitude of the overshoot is about 15–20% of the preceding main signal. Assuming that the FPP model is correct, this allows us to estimate the recollection of electrons by the antenna using equation (4) to be $Q_{ant} \geq 0.175 \times Q_{SC}C_{ant}/C_{SC} \approx 0.05 \times Q_{SC}$ or greater than about 5% of the charge collected by the SC. The $\geq$ sign is used to account for the fact that the charging time constants are short and the antennas are discharging even before the overshoots are revealed. The antenna discharge time constants in Figure 1b range from about 0.5 to 1.5 ms, which again compares well with $\tau_{ant} = 0.49$ ms from section 2. The antenna discharge time is in fact the strongest evidence supporting the FPP model. The different discharge time constants of the antennas could potentially be explained by different locations of the antennas relative to the SC body and thus exposed to a somewhat different environment (both illumination and influence of the spacecraft plasma sheath differ from antenna to antenna).

It is, however, important to take a closer look at the signals in order to identify features that are inconsistent with the FPP model. Two of these are the following: (1) there is a second overshoot occurring on the E_y antenna, making the measured signal positive again. There is no explanation for such feature in the model. (2) It is not uncommon that one of the antenna signals has a stronger main peak, which is then usually followed with a deeper overshoot as well (signal E_y in Figure 1b). The larger positive peak can only be explained by the particular antenna collecting fewer electrons from the impact plasma, while the larger overshoot peak would require an antenna collecting more electrons. These features do not contradict the FPP model directly, yet suggest the need for an additional mechanism that can generate overshoot signals.

Approximately 6% of the triple hits are inverted signals (Figure 1d). There are two possible scenarios for generating these subsets of events: (1) the SC is collecting dominantly positive charges, despite it being positively charged, or (2) the antennas collect the majority of impact-generated electrons. The latter could be explained by dust impacts occurring in the immediate vicinity of the antenna base, where the electrons from the impact plasma can be collected with high efficiency. The former scenario appears to be more plausible considering the shapes and discharge time constants of the initial peaks and that it would be difficult to collect consistently similar amounts of charge on the all three antennas. Net charge collection that is opposite in polarity to that preferred by applied bias voltages is occasionally observed in laboratory impact charge experiments (A. Collette, priv. communication); however, these were not statistically characterized and neither there is a good physical explanation for their occurrence. Again, the overshoots are of a typical shape, suggesting that they are generated by common mechanism.

A small subset of the triple-hit signals exhibits a preshoot (Figure 1(3)): a fast negative spike occurring right before the onset of the main signal. The preshoot is clearly not from charge collection as that can only discharge with longer time constants through the ambient plasma, as discussed above. Laboratory experiments provided two explanations for these features. Collette et al. (2015) found that for impacts in the vicinity of the antenna, the escaping electrons from the impact generated charge cloud can induce very similar "preshoot" signals. Nouzák et al. (2017) performed experiments investigating signal generation from both impacts on the SC and antenna. It was found that a preshoot can be generated also by the fast escape of the electrons from impact plasma, leaving thus behind a net positive charge that generates an induced signal. Either of these mechanisms appears to be plausible for generating the preshoots in Figure 1f.

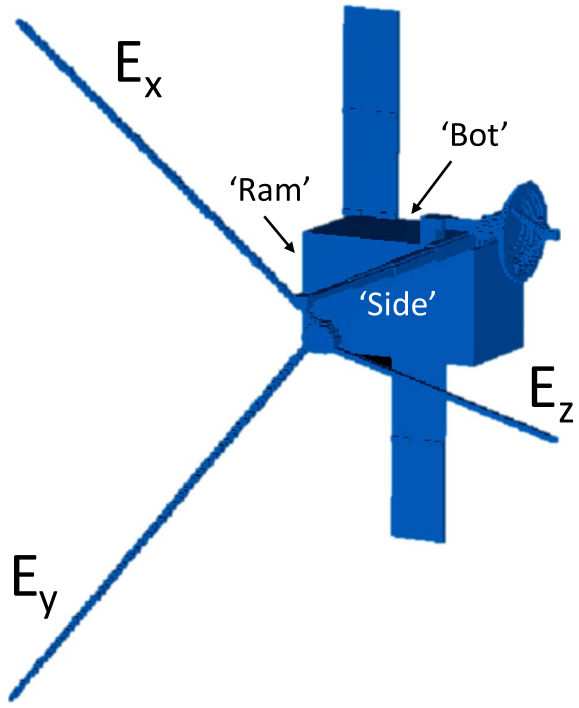

Figure 2. The reduced-size STEREO A spacecraft model used in collection efficiency calculations. Labels "bot," "ram," and "side" refer to faces with the assumed dust impacts. See text for more details.

Triple hit with single inverted and preshoot (Figure 1f) is a unique event that demonstrates how features of impact signals indeed can be interpreted with the help of analysis and laboratory simulations. This event can be interpreted as dust impact on antenna E_x. There is a clear and fast preshoot on this channel that is very similar to that reported by Nouzák et al. (2017) with the explanation provided above. The preshoot is followed by a negative-going signal that is due to collection of electrons by the antenna. Note that the discharge time constant of the main signal is visibly longer than those from impacts on the SC. The estimated discharge time constant of 0.36 ms compares well with $\tau_{ant} = 0.49$ ms from section 2. Another noteworthy feature is again the typical overshoot on E_x that clearly cannot be due to the FPP model. The positive (and shorter time scale!) signals on E_y and E_z suggest that the SC dominated the recollection of the impact plasma collection for those signals, and the different amplitudes suggest that E_z collected more electrons than E_y. Interestingly, it is E_y that has a pronounced overshoot, which again is in disagreement with the FPP model.

In summary, based on the number of inconsistencies listed above, it can be concluded that there appears to be a mechanism independent of the FPP model that generates the typical overshoots of the antenna signals. We leave it to a future investigation to determine this mechanism. Since the FPP model appears to be physically correct, a salient question is why are signatures of the FPP mechanism not more prominent in the data? The answer to this question is provided in section 4, namely, that the antennas are inefficient collectors of electrons from the impact plasma.

4. Numerical Modeling of Charge Recollection by the Antennas

One of the early analyses of the dust impact signals using antennas was performed by Gurnett et al. (1983) from the Voyager 2 Saturn encounter. This study concluded that antennas are able collectors of charge from the dust impact plasma with about 50% collection efficiency. Here we show that antennas are much less efficient in recollecting charged particles (electrons) from the impact plasma than is commonly believed.

The S/WAVES instrument detects dust signals in roughly the voltage range of 10–175 mV without saturating. Using equation (4), this equates to an impact charge collected by the SC in the range of $Q_I = \delta V C_{SC} = 2{\times}10^{-12} - 3.5 \times 10^{-11}$ C. The amplitude of the average dust impact signal from the statistical analysis in section 3 is about 50 mV, which corresponds to $Q_I = 1{\times}10^{-11}$ C. The impact plasma starts as a small, dense cloud of electrons and ions that is rapidly expanding. Based on recent laboratory measurements by Collette et al. (2016), the electron and ion temperatures of the impact plasma are in the range of 1–5 eV and 5–30 eV, respectively, with the ion temperatures increasing with impact speed. A simple estimate can be made to find the size of the expanding cloud when it can no longer be considered a plasma with its fast electrons coupled to the slower ions. The simplest model assumes a spherically symmetric plasma expanding into free space. The electrons, with higher thermal velocities, are retained in the cloud by the space charge of the slower ions, until the ion space charge drops below the electron temperature, $T_e/e_0 \geq \left(\frac{1}{4\pi\epsilon_0}\right)\frac{Q_I}{R}$, and the electrons can escape. (For completeness, we note that Meyer-Vernet et al. (2009) derived a similar relation by comparing the size of the cloud to the Debye length.) An average recorded dust impact event, using a conservative estimate of $T_e = 1$ eV, yields $R = 9$ cm as the upper limit for the size of the plasma cloud. Since this is much smaller than the characteristic dimensions of either the spacecraft or the antennas, it is physically more appropriate to think of the impact "plasma" as a decoupled cloud of fast-escaping and noninteracting electrons followed by an expanding cloud of slower ions. The trajectories of the charged particles from the impact plasma are then governed dominantly by the electrostatic electric fields of the SC-antenna system.

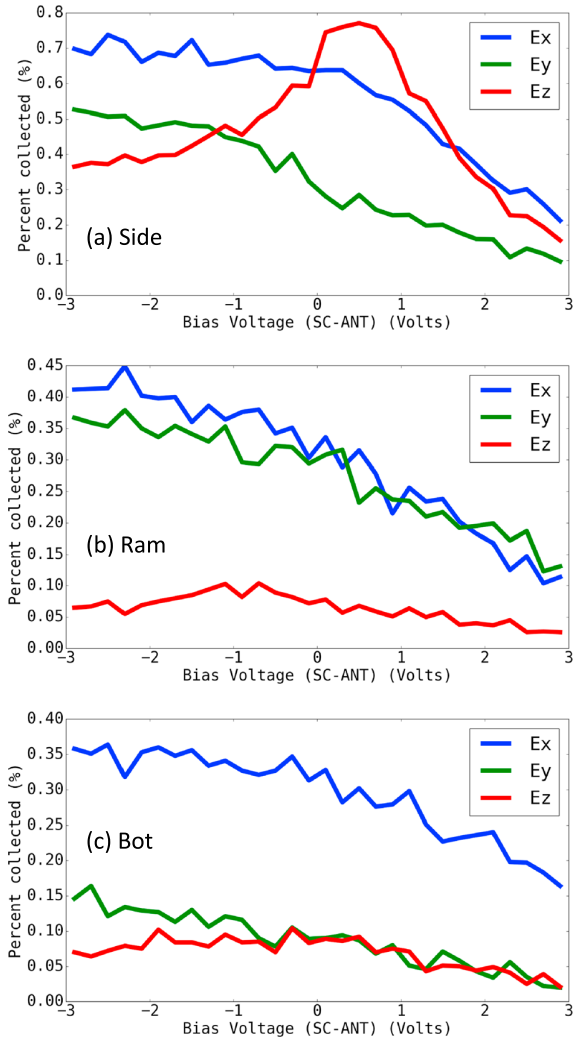

Figure 3. Antenna charge collection versus bias voltage (spacecraft-antenna) for each of the three antennas as a function of impact location defined in Figure 2.

This simple model allows a calculation of how efficient the antennas are in collecting electrons. To simulate this scenario, the SIMION software package (Manura & Dahl, 2008) is used. SIMION solves for the electrostatic potential of the SC/antenna system and calculates the trajectories of single particles by neglecting all other effects. The electrons are modeled as originating from a point source near the surface of the SC. They are launched with randomized velocities from a spherically symmetric 3-D distribution. Each component of the velocity is selected from Gaussian distribution centered around zero and with standard deviation of $(k_BT/m)^{1/2}$. When applied to the ensemble, this yields a Maxwell-Boltzmann energy distribution with an average energy of k_BT. Approximately 5 eV is assumed for the electron temperature.

Figure 2 shows a model of STEREO in SIMION with the SC body, solar panels, IMPACT boom, and three electric field antennas. The model is reduced in size to a 65:1 scale. Dust impact events are modeled to occur in the middle of three faces, labeled as "ram," "bot," and "side." The "ram" side is in the direction of the SC orbital velocity vector about the Sun, "bot" refers to the face toward the $-z$ direction in GSE coordinates, and "side" is where the antennas are mounted. The SC is held at a constant potential of +5 V, and the antenna biases are varied between 2 and 8 V. The effect of the Debye length of the ambient plasma is neglected as it is long compared to the characteristic size of the SC. The photoelectron sheath above the sunlit side of the SC is also neglected.

Figure 3 shows the calculated collection efficiencies of electrons by the antennas for the three impact locations. For each unique set of parameters, the trajectories of 10^5 electrons were followed and statistics established based on the number of electrons impacting the antennas. Not surprisingly, the largest collection efficiency is observed for dust impacts occurring on the closest face (side). Even then, the collection efficiency is only about 0.75% at most. Antennas E_x and E_y show an increasing collection efficiency with increasing positive bias potential. The antenna closest to the assumed dust impact location has a nontrivial variation with applied bias voltage, which is the result of the interplay of potentials from the other antennas. For impacts on the ram face, the antennas with a direct line of sight to the impact location (E_x and E_y) collect about 0.4% of the electrons for typical biasing conditions, while the antenna not directly visible from the impact location collects only about 0.1%. The situation is similar with impacts on the "bot" face, except that only antenna E_x is in the line of sight from the impact location. The reason why antennas not visible from the impact location have nonzero collection efficiencies is that electrons may orbit around the positive SC before reaching the antenna. In order to check that the model size was sufficiently large to simulate the collection efficiency of the antennas accurately, a second model with double size was constructed. The differences between the two models are on the order of the statistical uncertainties.

The results of recollection efficiencies are illustrative even for the highly reduced set of impact locations investigated. Clearly, there is a strong variation of collection efficiency with dust impact location. For impacts occurring from distant surfaces with no line of sight to the antenna(s), the collection efficiency will be very small, on the order of 0.1% and only weakly variable with antenna potential. In contrast, the measured triple-hit signals exhibit rather uniform ratios between the amplitudes of the overshoots and the preceding main signals (see section 3). Impacts very near the antenna base are not investigated, as for these, the assumptions made in the model are no longer valid for those impacts. Nevertheless, only a small fraction of dust particles would impact close enough to the antenna base, where the collection efficiency is considerably larger than 1%.

The collection efficiencies of ions are generally lower than for electrons. This is understandable as ions are more energetic and the positive bias on the SC and antennas reduce the collected fraction even further.

5. Conclusion and Summary

There are three main ideas that motivated this article. The first is, contrary to the common belief, antennas are poor collectors of charge from dust impact plasmas. This is certainly the case for the STEREO spacecraft and dust impact signals with amplitudes below saturation. The collection efficiency may be somewhat larger for the impact of larger (or faster) particles that generate substantially more impact plasma that could encompass significant parts of the antennas, but even then, the collection efficiency should be small. It is not surprising that the collection efficiency of the antennas is strongly dependent on the impact location, a fact that could be exploited to learn about the directionality of dust populations impacting the SC.

The second point is that it is important to analyze the entire data set of dust impact induced signals to draw correct conclusions. The FPP model appears valid for the subset of triple-hit signals. However, an analysis of the data that included atypical signals and the recognition of scaling laws within the subtypes of signals clearly showed that there ought to be yet another stronger mechanism responsible for the observed overshoots. Based on these results, the conclusion is that the FPP model, while physically correct, is not the dominant mechanism for the observed overshoots.

The third point to make is that it is a worthwhile effort to analyze the shapes of the dust impact signals and model them using known physical mechanisms. Supporting laboratory measurements are now available to provide the basic parameters of expanding plasma clouds from dust impacts, which can be utilized to calculate recollection rates on spacecraft and antennas as a function of floating potentials and impact locations. These calculations, combined with models of spacecraft in the ambient plasma environment, should be able to fully explain the shape of dust impact signals detected not only by the S/WAVES instruments but also for all other missions with antenna instruments sensitive to dust impacts. One of the remaining open issues is to clarify the mechanisms that generate the strong overshoot effects on STEREO and other missions.

Acknowledgments
All STEREO data used in this work are available from the STEREO/WAVES team at the following website: http://www.space.umn.edu/missions/stereo/. The digitized form of the data presented in Figure 3 is available upon request from coauthor Z. Sternovsky (zoltan.sternovsky@colorado.edu). The authors acknowledge the support from NASA through the IMPACT (Institute for Modeling Plasmas, Atmosphere and Cosmic Dust) node of the Solar System Exploration Research (SSERVI) program. Author E. O'Shea participated in this project through NSF's Research Experience for Undergraduates (REU) program.

References

Aubier, M., Meyer-Vernet, N., & Pedersen, B. M. (1983). Shot noise from grain and particle impacts in Saturn's ring plane. *Geophysical Research Letters*, *10*(1), 5–8. https://doi.org/10.1029/GL010i001p00005

Bale, S. D., Ullrich, R., Goetz, K., Alster, N., Cecconi, B., Dekkali, M., … Pulupa, M. (2008). The electric antennas for the STEREO/WAVES experiment. *Space Science Reviews*, *136*(1-4), 529–547. https://doi.org/10.1007/s11214-007-9251-x

Bougeret, J. L., Goetz, K., Kaiser, M. L., Bale, S. D., Kellogg, P. J., Maksimovic, M., … Zouganelis, I. (2008). S/WAVES: The radio and plasma wave investigation on the STEREO mission. *Space Science Reviews*, *136*(1-4), 487–528. https://doi.org/10.1007/s11214-007-9298-8

Collette, A., Grün, E., Malaspina, D., & Sternovsky, Z. (2014). Micrometeoroid impact charge yield for common spacecraft materials. *Journal of Geophysical Research: Space Physics*, *119*, 6019–6026. https://doi.org/10.1002/2014JA020042

Collette, A., Malaspina, D. M., & Sternovsky, Z. (2016). Characteristic temperatures of hypervelocity dust impact plasmas. *Journal of Geophysical Research: Space Physics*, *121*, 8182–8187. https://doi.org/10.1002/2015JA022220

Collette, A., Meyer, G., Malaspina, D., & Sternovsky, Z. (2015). Laboratory investigation of antenna signals from dust impacts on spacecraft. *Journal of Geophysical Research: Space Physics*, *120*, 5298–5305. https://doi.org/10.1002/2015JA021198

Czechowski, A., & Mann, I. (2010). Formation and acceleration of nano dust in the inner heliosphere. *The Astrophysical Journal*, *714*(1), 89–99. https://doi.org/10.1088/0004-637X/714/1/89

Gurnett, D. A., Grün, E., Gallagher, D., Kurth, W. S., & Scarf, F. L. (1983). Micron-sized particles detected near Saturn by the Voyager plasma wave instrument. *Icarus*, *53*(2), 236–254. https://doi.org/10.1016/0019-1035(83)90145-8

Gurnett, D. A., Kurth, W. S., Granroth, L. J., Allendorf, S. C., & Poynter, R. L. (1991). Micron-sized particles detected near Neptune by the Voyager 2 plasma wave instrument. *Journal of Geophysical Research*, *96*(S01), 19,177–19,187. https://doi.org/10.1029/91JA01270

Juhász, A., & Horányi, M. (2013). Dynamics and distribution of nano-dust particles in the inner solar system. *Geophysical Research Letters*, *40*(11), 2500–2504. https://doi.org/10.1002/grl.50535

Kellogg, P. J., Goetz, K., & Monson, S. J. (2016). Dust impact signals on the wind spacecraft. *Journal of Geophysical Research: Space Physics*, *121*, 966–991. https://doi.org/10.1002/2015JA021124

Kempf, S. (2008). Interpretation of high rate dust measurements with the Cassini dust detector CDA. *Planetary and Space Science*, *56*(3-4), 378–385, https://doi.org/10.1016/j.pss.2007.11.022

Kurth, W. S., Averkamp, T. F., Gurnett, D. A., & Wang, Z. (2006). Cassini RPWS observations of dust in Saturn's E ring. *Planetary and Space Science*, *54*(9-10), 988–998. https://doi.org/10.1016/j.pss.2006.05.011

Malaspina, D. M., O'Brien, L. E., Thayer, F., Sternovsky, Z., & Collette, A. (2015). Revisiting STEREO interplanetary and interstellardust flux and mass estimates. *Journal of Geophysical Research: Space Physics*, *120*, 6085–6100. https://doi.org/10.1002/2015JA021352

Manura, D., & Dahl, D. (2008). SIMION (R) 8.0 user manual. Scientific Instrument Services, Inc., Ringoes, NJ. Retrieved from http://simion.com

Meyer-Vernet, N., Aubier, M. G., & Pedersen, B. M. (1986). Voyager 2 at Uranus—Grain impacts in the ring plane. *Geophysical Research Letters*, *13*(7), 617–620. https://doi.org/10.1029/GL013i007p00617

Meyer-Vernet, N., Maksimovic, M., Czechowski, A., Mann, I., Zouganelis, I., Goetz, K., … Bale, S. D. (2009). Dust detection by the wave instrument on STEREO: Nanoparticles picked up by the solar wind? *Solar Physics*, *256*(1-2), 463–474. https://doi.org/10.1007/s11207-009-9349-2

Meyer-Vernet, N., Moncuquet, M., Issautier, K., & Lecacheux, A. (2014). The importance of monopole antennas for dust observations: Why Wind/WAVES does not detect nanodust. *Geophysical Research Letters*, *41*(8), 2716–2720. https://doi.org/10.1002/2014GL059988

Nouzák, L., Hsu, S., Malaspina, D., Thayer, F. M., Ye, S.-Y., Pavlu, J., … Sternovsky, Z. (2017). Laboratory modeling of dust impact detection by the Cassini spacecraft. *Planetary and Space Science*. https://doi.org/10.1016/j.pss.2017.11.014

O'Brien, L., Juhász, A., Horányi, M., & Sternovsky, Z. (2017). Effects of interplanetary coronal mass ejections on the transport of nano-dust generated in the inner solar system. *Planetary and Space Science*. https://doi.org/10.1016/j.pss.2017.11.013

Oberc, P. (1996). Electric antenna as a dust detector. *Advances in Space Research*, *17*(12), 105–110. https://doi.org/10.1016/0273-1177(95)00766-8

Pantellini, F., Belheouane, S., Meyer-Vernet, N., & Zaslavsky, A. (2012). Nano dust impacts on spacecraft and boom antenna charging. *Astrophysics and Space Science*, *341*, 309–314. https://doi.org/10.1007/s10509-012-1108-4

Pedersen, B. M., Meyer-Vernet, N., Aubier, M. G., & Zarka, P. (1991). Dust distribution around Neptune—Grain impacts near the ring plane measured by the Voyager planetary radio astronomy experiment. *Journal of Geophysical Research*, *96*(S01), 19,187–19,196. https://doi.org/10.1029/91JA01601

Sternovsky, Z., Chamberlin, P., Horanyi, M., Robertson, S., & Wang, X. (2008). Variability of the lunar photoelectron sheath and dust mobility due to solar activity. *Journal of Geophysical Research*, *113*(A10), A10104. https://doi.org/10.1029/2008JA013487

Thayer, F. M., Malaspina, D. M., Collette, A., & Sternovsky, Z. (2016). Variation in relative dust impact charge recollection with antenna to spacecraft potential on STEREO. *Journal of Geophysical Research: Space Physics*, *121*, 4998–5004. https://doi.org/10.1002/2015JA021983

Wang, Z., Gurnett, D. A., Averkamp, T. F., Persoon, A. M., & Kurth, W. S. (2006). Characteristics of dust particles detected near Saturn's ring plane with the Cassini radio and plasma wave instrument. *Planetary and Space Science*, *54*(9-10), 957–966. https://doi.org/10.1016/j.pss.2006.05.015

Ye, S.-Y., Gurnett, D. A., Kurth, W. S., Averkamp, T., Kempf, S., Hsu, H. W., … Grün, E. (2014). Properties of dust particles near Saturn inferred from voltage pulses induced by dust impacts on Cassini spacecraft. *Journal of Geophysical Research: Space Physics*, *119*, 6294–6312. https://doi.org/10.1002/2014JA020024

Ye, S.-Y., Gurnett, D. A., & Kurth, W. S. (2016). In-situ measurements of Saturn's dusty rings based on dust impact signals detected by Cassini RPWS. *Icarus*, *279*, 51–61. https://doi.org/10.1016/j.icarus.2016.05.006

Ye, S.-Y., Kurth, W. S., Hospodarsky, G. B., Averkamp, T. F., & Gurnett, D. A. (2016). Dust detection in space using the monopole and dipole electric field antennas. *Journal of Geophysical Research: Space Physics*, *121*, 11,964–11,972. https://doi.org/10.1002/2016JA023266

Zaslavsky, A. (2015). Floating potential perturbations due to micrometeoroid impacts: Theory and application to S/WAVES data. *Journal of Geophysical Research: Space Physics*, *120*, 855–867. https://doi.org/10.1002/2014JA020635

Zaslavsky, A., Meyer-Vernet, N., Mann, I., Czechowski, A., Issautier, K., Le Chat, G., … Kasper, J. C. (2012). Interplanetary dust detection by radio antennas: Mass calibration and fluxes measured by STEREO/WAVES. *Journal of Geophysical Research*, *117*, A05102. https://doi.org/10.1029/2011JA017480